MOLECULAR AND CELLULAR BIOLOGY, Oct. 2010, p. 4732–4743 Vol. 30, No. 19
0270-7306/10/$12.00 doi:10.1128/MCB.00413-10

BRCT Domain Interactions with Phospho-Histone H2A Target Crb2 to Chromatin at Double-Strand Breaks and Maintain the DNA Damage Checkpoint▽

Sevil Sofueva,[1] Li-Lin Du,[1]† Oliver Limbo,[1] Jessica S. Williams,[1]‡ and Paul Russell[1,2]*

Departments of Molecular Biology[1] and Cell Biology,[2] the Scripps Research Institute, La Jolla, California 92037

Received 9 April 2010/Returned for modification 13 May 2010/Accepted 19 July 2010

Relocalization of checkpoint proteins to chromatin flanking DNA double-strand breaks (DSBs) is critical for cellular responses to DNA damage. *Schizosaccharomyces pombe* Crb2, which mediates Chk1 activation by $Rad3^{ATR}$, forms ionizing radiation-induced nuclear foci (IRIF). Crb2 C-terminal BRCT domains ($BRCT_2$) bind histone H2A phosphorylated at a C-terminal SQ motif by $Tel1^{ATM}$ and $Rad3^{ATR}$, although the functional significance of this interaction is controversial. Here, we show that polar interactions of Crb2 serine-548 and lysine-619 with the phosphate group of phospho-H2A (γ-H2A) are critical for Crb2 IRIF formation and checkpoint function. Mutations of these $BRCT_2$ domain residues have additive effects when combined in a single allele. Combining either mutation with an allele that eliminates the threonine-215 cyclin-dependent kinase phosphorylation site completely abrogates Crb2 IRIF and function. We propose that cooperative phosphate interactions in the $BRCT_2$ γ-H2A-binding pocket of Crb2, coupled with tudor domain interactions with lysine-20 dimethylation of histone H4, facilitate stable recruitment of Crb2 to chromatin surrounding DSBs, which in turn mediates efficient phosphorylation of Chk1 that is required for a sustained checkpoint response. This mechanism of cooperative interactions with the γ-H2A/X phosphate is likely conserved in *S. pombe* Brc1 and human Mdc1 genome maintenance proteins.

Double-strand breaks (DSBs) are among the most dangerous forms of DNA damage (26, 30). Human cells experience DSBs several times a day, either during normal metabolism or as a consequence of exposure to DNA-damaging agents, such as ionizing radiation (IR) (18). Importantly, the unfaithful repair of such breaks can result in genome instability and cancer. The response to DSBs is coordinated by a conserved signal transduction cascade, which leads to cell cycle arrest and activation of DNA repair and constitutes the checkpoint response (9, 14, 20). The essential players in this process fall into four groups: sensors, mediators, transducers, and effectors (20). Sensors are the first to recognize and bind to DNA breaks and include the Mre11-Rad50-Nbs1 complex in humans and *Schizosaccharomyces pombe* (Mre11-Rad50-Xrs2 in *Saccharomyces cerevisiae*). The PIKKs (phosphoinositide 3-kinase-like kinases) ATR-ATRIP (ScMec1-ScDdc2/SpRad3-SpRad26) and ATM (ScTel1/SpTel1) act as transducers that transmit the signal to the effector kinases Chk1 (ScChk1/SpChk1) and Chk2 (ScRad53/SpCds1), whose role is to target downstream targets, such as p53 in mammals, and to amplify the signal (9, 14, 20).

Signaling between transducers and effectors is facilitated and enhanced by mediator proteins (19, 20). In the fission yeast *Schizosaccharomyces pombe*, Crb2/Rhp9 is a critical mediator of the DNA damage checkpoint (31, 42) and is related to *Saccharomyces cerevisiae* Rad9 and mammalian 53BP1 (p53 binding protein 1). $Rad3^{ATR}$-$Rad26^{ATRIP}$ phosphorylates Crb2 in response to damage, and Crb2 is required for phosphorylation of Chk1 by $Rad3^{ATR}$-$Rad26^{ATRIP}$ (31). Chk1, in turn, restrains entry into mitosis by phosphorylating and thus inactivating the phosphatase Cdc25 that is a mitotic inducer (10, 11, 28). Crb2-null cells are sensitive to a range of genotoxins and are unable to delay division in response to DNA damage (31, 42).

Crb2 is a nuclear protein that rapidly relocalizes to DSBs. This occurs on such a large scale that IR-induced nuclear foci (IRIF) of yellow fluorescent protein (YFP)-tagged Crb2 expressed from the endogenous promoter are readily detected by live cell microscopy (5). These foci colocalize with homologous recombination (HR) repair factors such as $Rad22^{Rad52}$. Two types of histone modifications regulate Crb2 localization at DSBs: C-terminal phosphorylation of histone H2A, denoted as γ-H2A (23), and lysine-20 dimethylation of histone H4, denoted as H4-K20me2 (32). Phosphorylation of an SQ motif within the C-terminal tail of histone H2A of budding yeast or fission yeast, or the H2AX variant in mammals, is one of the earliest cellular responses triggered by DNA damage (3, 23, 29). The γ-H2A/X modification, which is catalyzed by the checkpoint kinases ATR^{Rad3} and ATM^{Tel1}, spans large distances on both sides of a DSB, and it plays a critical role in recruiting DNA damage response proteins, chromatin remodeling complexes, and cohesin (2, 21, 23, 34, 35, 37, 38, 40). Protein crystallography and biochemical studies established that mammalian Mdc1, *S. pombe* Crb2, and Brc1 DNA damage response proteins directly bind the phosphorylated tail of histone H2A/X through tandem C-terminal BRCT domains (16, 35, 40). In contrast to γ-H2A, H4-K20 methylation catalyzed

* Corresponding author. Mailing address: Department of Molecular Biology, MB3, the Scripps Research Institute, 10550 North Torrey Pines Road, La Jolla, CA 92037. Phone: (858) 784-8273. Fax: (858) 784-2265. E-mail: prussell@scripps.edu.

† Present address: National Institute of Biological Sciences, 7 Science Park Road, Zhongguancun Life Science Park, Beijing 102206, China.

‡ Present address: Laboratory of Molecular Genetics, National Institute of Environmental Health Sciences Research, NIH, DHHS, Research Triangle Park, NC 27709.

▽ Published ahead of print on 2 August 2010.

by Set9/Kmt5 histone methyltransferase appears to be constitutive and not regulated by DNA damage (32). H4-K20me2 directly binds tandem tudor domains ($Tudor_2$) located to the N-terminal side of the BRCT domains in Crb2 (1).

YFP-Crb2 does not form IRIF in *hta1-S129A hta2-S128A* (*htaAQ*) or *rad3*Δ *tel1*Δ cells, in which γ-H2A phosphorylation is abolished (23), or in *set9*Δ cells or tudor domain mutants of Crb2 that ablate binding to H4-K20me2 (6, 32). However, Crb2 checkpoint functions are only partially impaired in an *htaAQ set9*Δ strain, implying that physiologically significant recruitment of Crb2 to DSBs also occurs by a histone modification-independent pathway. Indeed, we found that YFP-Crb2 forms microscopically visible foci in *htaAQ set9*Δ cells when DSBs are created by HO endonuclease or by treating cells in G_1 phase with IR (6). Unlike IR-induced DSBs formed during G_2 phase, these types of DSBs lack an intact sister chromatid that can be used for HR repair and therefore they are highly persistent. Further analysis revealed that the histone modification-independent pathway of recruiting Crb2 to DSBs requires threonine-215 (Thr215) phosphorylation catalyzed by the cyclin-dependent kinase (CDK) Cdc2, which facilitates an interaction with Cut5 (ScDpb11; mammalian TopBP1) (6, 8, 31). The *crb2-T215A* mutation does not ablate YFP-Crb2 IRIF formation; however, Crb2 Thr215 phosphorylation is required for formation of YFP-Crb2 foci at persistent DSBs in *htaAQ* or *set9*Δ cells, and combining *crb2-T215A* with *htaAQ* or *set9*Δ abolishes Crb2 function (6).

The tandem C-terminal BRCT domains ($BRCT_2$) of Crb2 not only mediate interactions with γ-H2A but also coordinate Crb2 homodimerization (4). In fact, replacing $BRCT_2$ with a leucine zipper (LZ) dimerization motif restores substantial function to Crb2 without restoring its ability to form IRIF. Thus, the most crucial task of the Crb2 BRCT domains is to provide a homodimerization platform, while binding to γ-H2A provides an additional function that is necessary for full resistance to DNA damage (4).

In a recent study, Kilkenny et al. (16) solved the crystal structures of Crb2-$BRCT_2$ alone and in complex with a γ-H2A-derived phosphopeptide containing the common C-terminal residues of H2A.1 and H2A.2 (the two H2A paralogues in *S. pombe*). These analyses revealed the structural determinants of $BRCT_2$ binding to γ-H2A and $BRCT_2$-mediated homodimerization of Crb2. Ser666 was found to be critical for homodimerization *in vitro*, and mutation of this residue severely impaired Crb2 function *in vivo*. Residues Ser548 and Lys619 were identified as important for the interaction with the phosphate group on γ-H2A.1 pSer129. However, a charge reversal mutation of Lys619 did not abrogate Crb2 IRIF formation measured using methanol-fixed cells, although it did disrupt binding to a γ-H2A peptide *in vitro* (16). These unexpected findings indicated that γ-H2A likely has an indirect role in regulating Crb2 localization at DSBs. Here, we investigate Crb2 localization in live cells and find that while mutations of Ser548 or Lys619 partially impair Crb2 IRIF, the corresponding double mutant is severely deficient in Crb2 IRIF formation. Our findings and an independent study by Sanders et al. (33) show that γ-H2A binding to $BRCT_2$ is critical for Crb2 focus formation at IR-induced DSBs and for maintaining a DNA damage checkpoint response.

MATERIALS AND METHODS

Yeast strains. The strains used in this study are described in Table 1. Point mutations were created using the QuikChange XL site-directed mutagenesis kit from Stratagene. Constructs with two tandem copies of YFP inserted behind the start codon of the *crb2* ORF (5) were linearized with NruI and integrated into the *leu1-32* locus of a *crb2*Δ::*ura4*$^+$ or a *crb2*Δ::*kanMX* mutant (the carrier plasmid containing the *leu1*$^+$ marker, pJK148, is described in reference 15). In these constructs Crb2 is expressed from the endogenous *crb2*$^+$ promoter (all the intergenic sequences between *crb2*$^+$ and its neighboring genes have been cloned upstream and downstream of the 2YFP-tagged construct). Transformants were selected on minimal medium (EMM) lacking leucine and subsequently checked for growth on medium lacking uracil or on kanamycin (G418) plates. To ensure the plasmid was integrated, cells were grown on complete medium (YES) plates and replica plated onto a selective medium. For each experiment, the strains used were ensured to be with equal levels of 2YFP-Crb2 expression by microscopically observing background nuclear fluorescence. The YFP tag does not affect the functionality of Crb2 (5; S. Sofueva and P. Russell, unpublished data). To test the effects of DSBs created by the HO endonuclease, strains harboring the HO cleavage site tagged with a kanamycin resistance cassette within the *arg3* locus and expressing the HO endonuclease from the thiamine-repressible *nmt41* promoter were used (5, 6). HO expression was downregulated by adding 5 μM thiamine (vitamin B1) to minimal medium or growing the strains on complete medium, which already contains B1.

Genotoxin sensitivity assays. To assess genotoxin sensitivity, cultures were grown to log phase (optical density at 600 nm [OD_{600}], 0.4 to 0.8) and serial 1:5 dilutions were spotted onto control and genotoxin plates. For IR survival curves, log-phase cultures were irradiated with a GammaCell-1000 (~2.75 Gy/min) and cells were plated in triplicate on YES plates.

Microscopy. Cells were maintained in logarithmic phase (OD_{600}, 0.4 to 0.8) in EMM minimal medium at 25°C for approximately 48 h prior to irradiation or mock irradiation (6). Images of Crb2 IRIF were obtained using a DeltaVision optical sectioning microscope model 283 equipped with a YFP/cyan fluorescent protein (CFP)/red fluorescent protein (RFP) filter set and a Photometrics CH350L cooled charge-coupled-device camera. A 60× 1.4 NA objective was used and 15 to 20 z-sections at 0.2-μm intervals were photographed and deconvolved using the soft WoRx software. The z-stacks were compressed to a maximal projection using the Imaris 6.4.2 software (Bitplane Scientific Software) or ImageJ (NIH). For time course experiments, between 150 and 200 cells were counted for each time point. Each experiment was done at least twice.

To visualize 2YFP-Crb2 and Rad22-2CFP (cyan fluorescent protein) recruitment to an HO break, cells were grown on minimal medium lacking B1 at 25°C for 27 h. Then, 8 z-sections at 0.5-μm intervals were photographed and deconvolved.

Cell cycle analysis. Strains carrying the *cdc25-22* mutation were synchronized by a temperature shift to 35.5°C for 2.5 h. During irradiation, samples were kept in a thermos with 35-degree water (Aladdin Migo). After irradiation, cells were released into fresh YES at 25°C. Samples for microscopy were taken every 20 min and fixed with 70% ethanol. Cells were stained with Calcofluor to visualize the septum (7).

Western blots. Whole-cell extracts were prepared from exponentially growing cultures using a bead-beater (described in reference 22). To assess Chk1 phosphorylation, strains expressing Chk1-9myc2HA6His were used. Samples were run on 8% acrylamide-bisacrylamide gels. Western blots were probed with a mouse monoclonal anti-HA antibody from Roche (clone 12CA5). The secondary antibody was horseradish peroxidase (HRP)-conjugated goat anti-mouse antibody from Pierce Biotechnology (31430). Bands were quantified with ImageJ (NIH) using TIFF files of scanned X-ray films with similar exposure times.

RESULTS

Crb2 IRIF form independently of Brc1. We previously found that γ-H2A is required for Crb2 IRIF formation and a fully proficient checkpoint response, that replacing the Crb2 BRCT-domains with a LZ dimerization domain partially restores DNA damage resistance without restoring IRIF, and that Crb2 binds a γ-H2A C-terminal phosphopeptide *in vitro* (4, 6, 23, 24). From these and other data we proposed that $BRCT_2$ binding to γ-H2A mediates Crb2 IRIF formation. The crystal structure of Crb2-$BRCT_2$ bound to a γ-H2A phosphopeptide revealed the structural determinants of Crb2 binding to γ-H2A

TABLE 1. *S. pombe* strains used in this study

Strain	Mating type	Genotype	Source or reference
LLD3259	*h*$^-$	*crb2Δ::ura4*$^+$ *leu1-32 ura4-D18*	5
LLD3260	*h*$^-$	*leu1-32::2YFP-crb2*$^+$*-leu1*$^+$ *crb2Δ::ura4*$^+$ *ura4-D18*	5
LLD3495	*h*$^-$	*leu1-32::2YFP-crb2(1-520)-leu1*$^+$ *crb2Δ::ura4*$^+$ *ura4-D18*	4
LLD3496	*h*$^-$	*leu1-32::2YFP-crb2(1-520)-LZ-leu1*$^+$ *crb2Δ::ura4*$^+$ *ura4-D18*	4
LLD3628	*h*$^-$	*crb2Δ::ura4*$^+$ *leu1-32 ura4-D18 his3-D1 cdc25-22*	6
LLD3643	*h*$^-$	*leu1-32::2YFP-crb2-F400A-leu1*$^+$ *crb2Δ::ura4*$^+$ *ura4-D18 his3-D1*	6
LLD3650	*h*$^-$	*leu1-32::2YFP-crb2*$^+$*-leu1*$^+$ *crb2Δ::ura4*$^+$ *rad22*$^+$*-2CFP-kanMX ura4-D18 his3-D1 arg3::HOsite-kanMX ars1::nmt41promoter-HO-his3*$^+$	6
LLD3652	*h*$^-$	*leu1-32::2YFP-crb2*$^+$*-leu1*$^+$ *crb2Δ::ura4*$^+$ *rad22*$^+$*-2CFP-kanMX ura4-D18 his3-D1 arg3::HOsite-kanMX ars1::nmt41promoter-HO-his3*$^+$ *hta1-S129A::ura4*$^+$ *hta2-S128A::kanMX*	6
LLD4897	*h*$^-$	*leu1-32::2YFP-crb2-T215A-leu1*$^+$ *crb2Δ::ura4*$^+$ *ura4-D18*	This study
LLD4898	*h*$^-$	*leu1-32::2YFP-crb2*$^+$*-leu1*$^+$ *crb2Δ::ura4*$^+$ *ura4-D18 his3-D1 hta1-S129A::ura4*$^+$ *hta2-S128A::his3*$^+$	This study
LLD4899	*h*$^+$	*leu1-32::2YFP-crb2-T215A crb2Δ::ura4*$^+$ *ura4-D18 his3-D1 hta1-S129A::ura4*$^+$ *hta2-S128A::his3*$^+$	This study
LLD4900	*h*$^+$	*leu1-32::2YFP-crb2-T215A-leu1*$^+$ *crb2Δ::ura4*$^+$ *rad22*$^+$*-2CFP-kanMX ura4-D18 his3-D1 arg3::HOsite-kanMX ars1::nmt41promoter-HO-his3*$^+$	This study
LLD4901	*h*$^-$	*leu1-32::2YFP-crb2-S548A-leu1*$^+$ *crb2Δ::ura4*$^+$ *ura4-D18 his3-D1*	This study
LLD4902	*h*$^-$	*leu1-32::2YFP-crb2-K619M-leu1*$^+$ *crb2Δ::ura4*$^+$ *ura4-D18 his3-D1*	This study
OL4925	*h*$^-$	*chk1-9myc2HA6His::ura4*$^+$ *crb2Δ::kanMX leu1-32::2YFP-crb2*$^+$*-leu1*$^+$ *ura4-D18 hta1-S129A::ura4*$^+$ *hta2-S128A::his3*$^+$	This study
OL4926	*h*$^-$	*chk1-9myc2HA6His::ura4*$^+$ *crb2Δ::kanMX leu1-32::2YFP-crb2-S548A-leu1*$^+$ *ura4-D18 hta1-S129A::ura4*$^+$ *hta2-S128A::his3*$^+$	This study
OL4927	*h*$^-$	*chk1-9myc2HA6His::ura4*$^+$ *crb2Δ::kanMX leu1-32::2YFP-crb2-K619M-leu1*$^+$ *ura4-D18 hta1-S129A::ura4*$^+$ *hta2-S128A::his3*$^+$	This study
OL4928	*h*$^-$	*chk1-9myc2HA6His::ura4*$^+$ *crb2Δ::kanMX leu1-32::2YFP-crb2-S548AK619M-leu1*$^+$ *ura4-D18 hta1-S129A::ura4*$^+$ *hta2-S128A::his3*$^+$	This study
OL4929	*h*$^+$	*leu1-32::2YFP-crb2-K619M-leu1*$^+$ *crb2Δ::ura4*$^+$ *rad22*$^+$*-2CFP-kanMX ura4-D18 his3-D1 arg3::HOsite-kanMX ars1::nmt41promoter-HO-his3*$^+$ *hta1-S129A::ura4*$^+$ *hta2-S128A::kanMX*	This study
OL4930	*h*$^+$	*leu1-32::2YFP-crb2-K619M-leu1*$^+$ *crb2Δ::ura4*$^+$ *rad22*$^+$*-2CFP-kanMX ura4-D18 his3-D1 arg3::HOsite-kanMX ars1::nmt41promoter-HO-his3*$^+$	This study
OL4931	*h*$^+$	*leu1-32::2YFP-crb2-S548AK619M-leu1*$^+$ *crb2Δ::ura4*$^+$ *rad22*$^+$*-2CFP-kanMX ura4-D18 his3-D1 arg3::HOsite-kanMX ars1::nmt41promoter-HO-his3*$^+$	This study
OL4932	*h*$^+$	*leu1-32::2YFP-crb2-S548AK619M-leu1*$^+$ *crb2Δ::ura4*$^+$ *rad22*$^+$*-2CFP-kanMX ura4-D18 his3-D1 arg3::HOsite-kanMX ars1::nmt41promoter-HO-his3*$^+$ *hta1-S129A::ura4*$^+$ *hta2-S128A::kanMX*	This study
YJW4896	*h*$^-$	*leu1-32::2YFP-crb2*$^+$*-leu1*$^+$ *crb2Δ::ura4*$^+$ *brc1Δ::hphMX ura4-D18*	This study
SAS4903	*h*$^-$	*leu1-32::2YFP-crb2-T215AS548A-leu1*$^+$ *crb2Δ::ura4*$^+$ *ura4-D18*	This study
SAS4904	*h*$^-$	*leu1-32::2YFP-crb2*$^+$*-leu1*$^+$ *crb2Δ::ura4*$^+$ *ura4-D18 cdc25-22*	This study
SAS4905	*h*$^-$	*leu1-32::2YFP-crb2-S548A-leu1*$^+$ *crb2Δ::ura4*$^+$ *ura4-D18 cdc25-22*	This study
SAS4906	*h*$^-$	*leu1-32::2YFP-crb2-K619M-leu1*$^+$ *crb2Δ::ura4*$^+$ *ura4-D18 cdc25-22*	This study
SAS4907	*h*$^-$	*leu1-32::2YFP-crb2-S548AK619M-leu1*$^+$ *crb2Δ::ura4*$^+$ *ura4-D18*	This study
SAS4908	*h*$^-$	*leu1-32::2YFP-crb2-S548AK619M-leu1*$^+$ *crb2Δ::ura4*$^+$ *ura4-D18*	This study
SAS4909	*h*$^-$	*chk1-9myc2HA6His::ura4*$^+$ *crb2Δ::kanMX leu1-32 ura4-D18*	This study
SAS4910	*h*$^-$	*chk1-9myc2HA6His::ura4*$^+$ *crb2Δ::kanMX leu1-32::2YFP-crb2-S548A-leu1*$^+$ *ura4-D18*	This study
SAS4911	*h*$^-$	*chk1-9myc2HA6His::ura4*$^+$ *crb2Δ::kanMX leu1-32::2YFP-crb2-K619M-leu1+ ura4-D18*	This study
SAS4912	*h*$^-$	*chk1-9myc2HA6His::ura4*$^+$ *crb2Δ::kanMX leu1-32::2YFP-crb2-T215AS548A-leu1*$^+$ *ura4-D18*	This study
SAS4913	*h*$^-$	*chk1-9myc2HA6His::ura4*$^+$ *crb2Δ::kanMX leu1-32::2YFP-crb2-S548AK619M-leu1*$^+$ *ura4-D18*	This study
SAS4914	*h*$^-$	*chk1-9myc2HA6His::ura4*$^+$ *crb2Δ::kanMX leu1-32::2YFP-crb2*$^+$*-leu1*$^+$ *ura4-D18*	This study
SAS4915	*h*$^-$	*chk1-9myc2HA6His::ura4*$^+$ *crb2Δ::kanMX leu1-32::2YFP-crb2-T215A-leu1*$^+$ *ura4-D18*	This study
SAS4916	*h*$^-$	*leu1-32::2YFP-crb2-T215AK619M-leu1*$^+$ *crb2Δ::ura4*$^+$ *ura4-D18*	This study
SAS4917	*h*$^-$	*leu1-32::2YFP-crb2-S548AK619M-leu1*$^+$ *crb2::ura4*$^+$ *ura4-D18 cdc25-22*	This study
SAS4918	*h*$^+$	*leu1-32::2YFP-crb2-S548A-leu1*$^+$ *crb2Δ::ura4*$^+$ *rad22*$^+$*-2CFP-kanMX ura4-D18 his3-D1 arg3::HOsite-kanMX ars1::nmt41promoter-HO-his3*$^+$	This study
SAS4919	*h*$^+$	*leu1-32::2YFP-crb2-T215AS548A-leu1*$^+$ *crb2Δ::ura4*$^+$ *rad22*$^+$*-2CFP-kanMX ura4-D18 his3-D1 arg3::HOsite-kanMX ars1::nmt41promoter-HO-his3*$^+$	This study
SAS4920	*h*$^-$	*leu1-32::2YFP-crb2-S548AK619M-leu1*$^+$ *crb2Δ::ura4*$^+$ *ura4-D18 his3-D1 hta1-S129A::ura4*$^+$ *hta2-S128A::his3*$^+$	This study
SAS4921	*h*$^-$	*leu1-32::2YFP-crb2-K619M-leu1*$^+$ *crb2Δ::ura4*$^+$ *ura4-D18 his3-D1 hta1-S129A::ura4*$^+$ *hta2-S128A::his3*$^+$	This study
SAS4922	*h*$^-$	*leu1-32::2YFP-crb2-T215A-leu1*$^+$ *crb2Δ::ura4*$^+$ *brc1Δ::hphMX ura4-D18*	This study
SAS4923	*h*$^-$	*leu1-32::2YFP-crb2-S548A-leu1*$^+$ *crb2Δ::ura4*$^+$ *brc1Δ::hphMX ura4-D18*	This study
SAS4924	*h*$^+$	*leu1-32::2YFP-crb2-K619M-leu1*$^+$ *crb2Δ::ura4*$^+$ *brc1Δ::hphMX ura4-D18*	This study
SAS4933	*h*$^-$	*leu1-32::2YFP-crb2*$^+$*-leu1*$^+$ *crb2Δ::ura4*$^+$ *ura4-D18*	This study
SAS4934	*h*$^-$	*leu1-32::2YFP-crb2-K619M-leu1*$^+$ *crb2Δ::ura4*$^+$ *ura4-D18*	This study
SAS4935	*h*$^-$	*leu1-32::2YFP-crb2-F400A-leu1*$^+$ *crb2Δ::ura4*$^+$ *ura4-D18*	This study
SAS4936	*h*$^-$	*leu1-32::2YFP-crb2-F400AK619M-leu1*$^+$ *crb2Δ::ura4*$^+$ *ura4-D18*	This study
SAS4937	*h*$^-$	*leu1-32::2YFP-crb2-F400AS548AK619M-leu1*$^+$ *crb2Δ::ura4*$^+$ *ura4-D18*	This study
SAS4938	*h*$^-$	*chk1-9myc2HA6His::ura4*$^+$ *crb2Δ::kanMX leu1-32::2YFP-crb2-F400A-leu1*$^+$ *ura4-D18*	This study
SAS4939	*h*$^-$	*chk1-9myc2HA6His::ura4*$^+$ *crb2Δ::kanMX leu1-32::2YFP-crb2-F400AS548A-leu1*$^+$ *ura4-D18*	This study
SAS4940	*h*$^-$	*chk1-9myc2HA6His::ura4*$^+$ *crb2Δ::kanMX leu1-32::2YFP-crb2-F400AK619M-leu1*$^+$ *ura4-D18*	This study
SAS4941	*h*$^-$	*chk1-9myc2HA6His::ura4*$^+$ *crb2Δ::kanMX leu1-32::2YFP-crb2-F400AS548AK619M-leu1*$^+$ *ura4-D18*	This study
SAS4942	*h*$^-$	*leu1-32::2YFP-crb2-F400AS548A-leu1*$^+$ *crb2Δ::ura4*$^+$ *ura4-D18*	This study

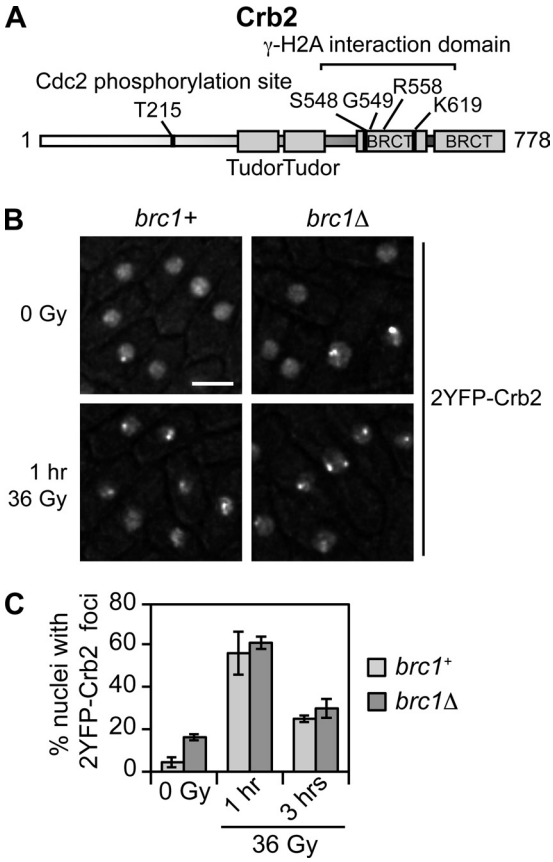

FIG. 1. Crb2 forms IRIF independently of Brc1. (A) Domain organization of Crb2. Tandem tudor domains, which are conserved in mammalian 53BP1 DNA damage response protein, bind histone H4-K20me2 and are required for Crb2 IRIF formation (1, 32). The phosphate group of γ-H2A.1 pSer129 binds in a small pocket of Crb2-$BRCT_2$ and makes polar contacts with the main and side chains of Ser548 and Lys619 (16). These contacts have direct functional counterparts in mammalian Mdc1 (35). The crystal structure of Crb2-$BRCT_2$ in complex with the γ-H2A.1 pSer129 peptide also identified contacts between the phosphate and the peptide nitrogen of Gly549 and a water-bridged interaction with Arg558 (16). Residue Thr215 is a Cdc2 (CDK) phosphorylation site important for proper checkpoint response but not for IRIF formation (8, 24). (B) Crb2 IRIF in asynchronous *brc1*$^+$ and *brc1*Δ cells irradiated with 36 Gy IR. 2YFP-Crb2 localization was observed 1 h (shown) and 3 h after irradiation. Bar, 5 μm. (C) Quantification of the percentage of nuclei with 2YFP-Crb2 foci. A total of 150 nuclei were scored for each time point. Error bars represent results of three independent experiments. The strains used are LLD3260 (*brc1*$^+$) and YJW4896 (*brc1*Δ).

and BRCT-mediated homodimerization of Crb2 (16). The phosphate group of γ-H2A.1 pSer129 formed well-ordered polar interactions with Ser548, Lys619, and the main chain nitrogen of Gly549, in addition to a water-bridged interaction with the side chain of Arg558 of Crb2 (Fig. 1A). Ser548 and Lys619 appeared to be particularly important, as they have direct functional counterparts in the C-terminal BRCT domains of mammalian Mdc1 and *S. pombe* Brc1 that contact the phosphate group of γ-H2A/X (35, 40). Indeed, a charge reversal mutation of Lys619 into Glu (*crb2-K619E*) abrogated Crb2-$BRCT_2$ binding to a γ-H2A peptide *in vitro* (16).

Surprisingly, microscopic analysis of methanol-fixed cells indicated that *crb2-K619E* does not affect Crb2 IRIF (16). In an attempt to reconcile this result with evidence that γ-H2A is required for Crb2 IRIF, we considered whether γ-H2A has an indirect role in mediating Crb2 IRIF. Through X-ray crystallography, biochemistry, and genetics, we recently found that the *S. pombe* DNA damage response protein Brc1 directly binds γ-H2A through its C-terminal BRCT domains (40). This interaction is required for formation of Brc1 IRIF. Furthermore, we found that Brc1 and Crb2 colocalize in IRIF, and Brc1 foci form independently of Crb2 (40). These observations suggested a model in which Brc1 binding to γ-H2A might be required for Crb2 IRIF. This hypothesis could explain why γ-H2A is required for Crb2 IRIF and yet the *crb2-K619E* mutation that disrupts Crb2 binding to γ-H2A does not abrogate Crb2 IRIF. To test this model, instead of analyzing methanol-fixed cells (16), we monitored YFP-tagged Crb2 in *brc1*$^+$ and *brc1*Δ strains by live cell microscopy using a DeltaVision optical sectioning microscope (Fig. 1B) (5). For this study wild-type or mutant constructs (see below) of genomic *crb2* flanked by upstream and downstream intergenic regions were integrated into the *leu1-32* locus in a *crb2*Δ background (5). As seen previously (5), the 2YFP tag did not noticeably affect Crb2 function in genotoxin sensitivity assays (Sofueva and Russell, unpublished). Approximately 4% of wild-type cells in a log-phase culture had 2YFP-Crb2 foci, while in the *brc1*Δ background the frequency of 2YFP-Crb2 foci was about 4-fold higher (~16%). This difference is consistent with our studies showing that *brc1*Δ cells have an increased incidence of Rad22-YFP HR repair foci (40). In response to exposure to 36 Gy IR, wild-type and *brc1*Δ cells displayed similar levels of 2YFP-Crb2 IRIF (Fig. 1B and C). Thus, Crb2 forms IR-induced foci independently of Brc1.

$BRCT_2$ binding to γ-H2A is critical for Crb2 focus formation in irradiated cells. As Brc1 and Crb2 are the only proteins known to have physiologically significant binding to γ-H2A in *S. pombe*, we decided to reevaluate the role of Crb2-$BRCT_2$ binding to γ-H2A in the formation of Crb2 IRIF. We monitored 2YFP-Crb2 foci in live cells (Fig. 2A). 2YFP-Crb2 foci were detected in ~1 to 4% of wild-type nuclei prior to IR exposure (Fig. 2B and C). This value increased to ~60% of nuclei at the 0- and 1-h time points following exposure to 36 Gy IR (Fig. 2B). These absolute levels of nuclei with Crb2 foci are somewhat lower than previously reported (6), which may be due to differences in the media and/or growth conditions, but the overall patterns are very similar. As expected, Crb2 IRIF were almost eliminated in the *htaAQ* mutant (~5% of nuclei 0 to 1 h post-IR), while the *crb2-T215A* mutation had little effect (Fig. 2A and B). In contrast to *crb2-T215A*, the *S548A* and *K619M* mutations in the γ-H2A phosphopeptide-binding pocket of Crb2-$BRCT_2$ strongly impaired Crb2 IRIF, reducing the value to ~20% of nuclei at 0 to 1 h post-IR (Fig. 2A and B).

As the effects of the *S548A* and *K619M* mutations on Crb2 IRIF were weaker than *htaAQ*, we considered whether these mutations might not fully abrogate Crb2-$BRCT_2$ interactions with γ-H2A *in vivo*. To address this possibility, we constructed and expressed a 2YFP-Crb2 construct harboring both mutations. Indeed, the *crb2-S548AK619M* allele almost completely eliminated Crb2 IRIF, being quite similar to the *htaAQ* mutant (Fig. 2A and B). From these data we conclude that Ser548 and

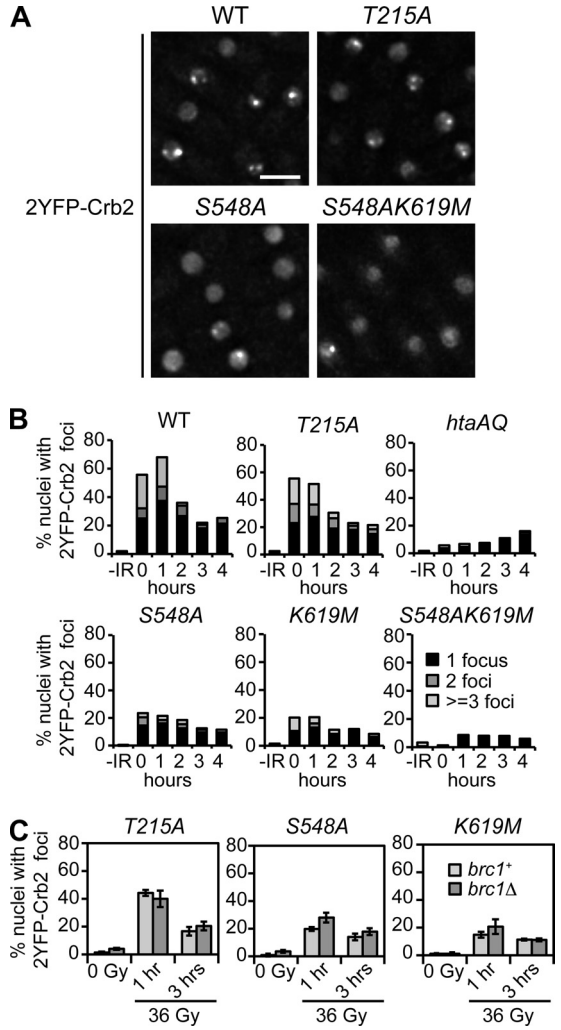

FIG. 2. Crb2 focus induction by IR is largely dependent on the interaction with γ-H2A. (A) Representative images of 2YFP-Crb2 localization in IR-treated cells 1 h post-irradiation with 36 Gy. Bar, 5 μm. WT, wild type. (B) Quantitative representation of the numbers of foci in the different mutants. Exponentially growing asynchronous cultures were subjected to 36 Gy IR and nuclei with 1, 2, or more foci were counted as a percentage of the total. Each experiment was done at least twice. About 200 nuclei were scored for each time point. (C) Quantification of IR-iduced focus formation (36 Gy) by Crb2 point mutants in *brc1*Δ cells. A total of 150 nuclei were scored for each time point. Error bars represent three independent experiments. The strains used for the experiments shown in this figure are LLD3260 (*crb2*$^+$), LLD4897 (*crb2-T215A*), LLD4898 (*hta-AQ*), LLD4901 (*crb2-S548A*), LLD4902 (*crb2-K619M*), SAS4908 (*crb2-S548AK619M*), SAS4922 (*crb2-T215A brc1*Δ), SAS4923 (*crb2-S548A brc1*Δ), and SAS4924 (*crb2-K619M brc1*Δ).

Lys619 seem to independently interact with the pSer129 phosphate group of γ-H2A.1, and thus it is necessary to disrupt both interactions to fully ablate Crb2-BRCT$_2$ binding to γ-H2A.

Weakening of γ-H2A binding to Crb2-BRCT$_2$ does not result in a requirement for Brc1 for Crb2 IRIF formation. We next investigated whether weaker binding of Crb2 to γ-H2A in the *crb2-S548A* and *crb2-K619M* mutants might expose a role for Brc1 in Crb2 IRIF formation. We compared the percentage of cells with IRIF at 1 h and 3 h following treatment with 36 Gy IR (Fig. 2C). In addition to the Crb2-BRCT$_2$ point mutants, we also tested the *crb2-T215A* strain. Only minor differences in the levels of 2YFP-Crb2 foci between *brc1*$^+$ and *brc1*Δ cells were detected (Fig. 2C). These data reinforce the conclusion that Brc1 does not have a role in Crb2 recruitment to sites of DNA damage.

Crb2-BRCT$_2$ interactions with γ-H2A are required for full resistance to DNA-damaging agents. We previously found that *htaAQ* cells are modestly sensitive to a range of genotoxins, with the largest effects seen with the topoisomerase I inhibitor CPT, which causes replication fork collapse (6, 23). We compared the genotoxin sensitivities of our BRCT mutants to that of *htaAQ* cells. Cells were subjected to chronic exposure to CPT, to the DNA alkylating agent MMS, which also collapses replication forks, to the DNA replication inhibitor HU, which depletes deoxynucleoside triphosphate (dNTP) pools, or to an acute exposure to UV (Fig. 3A). Mutating Lys619 or Ser548 alone had weak effects in the doses used for these experiments (Fig. 3A). However, combining these mutations enhanced genotoxin sensitivity. This was particularly apparent for MMS and higher doses of CPT (Fig. 3A; also see Fig. 3C). In MMS or CPT assays, the *htaAQ* cells were more sensitive than *crb2-S548AK619M* cells, which is consistent with our genetic epistasis studies showing that Brc1 binding to γ-H2A plays an important Crb2-independent role in the survival of replication-associated DNA damage (40). We also found that *crb2-S548AK619M* cells displayed enhanced IR sensitivity relative to the wild type (Fig. 3B).

The enhanced genotoxin sensitivity of *crb2-S548AK619M* cells relative to *S548A* or *K619M* cells is consistent with the Crb2 IRIF studies, in which the double mutant allele shows a greater defect (see Fig. 2A and B). To extend these studies, we compared the 5 μM CPT sensitivity of representative mutants to the *crb2*(*1-520*) mutant, which lacks the entire C-terminal region containing the tandem BRCT domains, and *crb2*(*1-520*)*-LZ*, which has Crb2-BRCT$_2$ substituted with a leucine zipper dimerization domain (4). The *crb2*(*1-520*) cells were as sensitive as *crb2*Δ cells, confirming that the BRCT domains are essential for Crb2 function (Fig. 3C). CPT resistance was substantially improved in *crb2*(*1-520*)*-LZ* cells, underlining the importance of BRCT$_2$ homodimerization for the functionality of Crb2 (4, 16). The *crb2*(*1-520*)*-LZ* and *crb2-S548AK619M* cells were similarly sensitive to CPT, as expected if the BRCT$_2$ mutations ablate γ-H2A binding while maintaining BRCT domain homodimerization (Fig. 3C). A very similar pattern was observed with 0.01% MMS, although *crb2*(*1-520*)*-LZ* cells were slightly more sensitive than *crb2-S548AK619M* cells, indicating that leucine zipper dimerization does not fully replicate the functionality of BRCT domain homodimerization (Fig. 3C).

Thr215 phosphorylation and γ-H2A binding independently affect Crb2 function. Crb2 localizes to DSBs via two pathways: one requiring γ-H2A and H4-K20me2 histone modifications and the other requiring Crb2 Thr215 phosphorylation. If, as our data suggest, the *crb2-S548A* and *-K619M* mutations impair the pathway mediated by γ-H2A, we would expect these mutations to show phenotypic enhancement interactions with the *crb2-T215A* mutation. Accordingly, we introduced the *htaAQ*, *crb2-S548A*, or *crb2-K619M* mutations into the *crb2-*

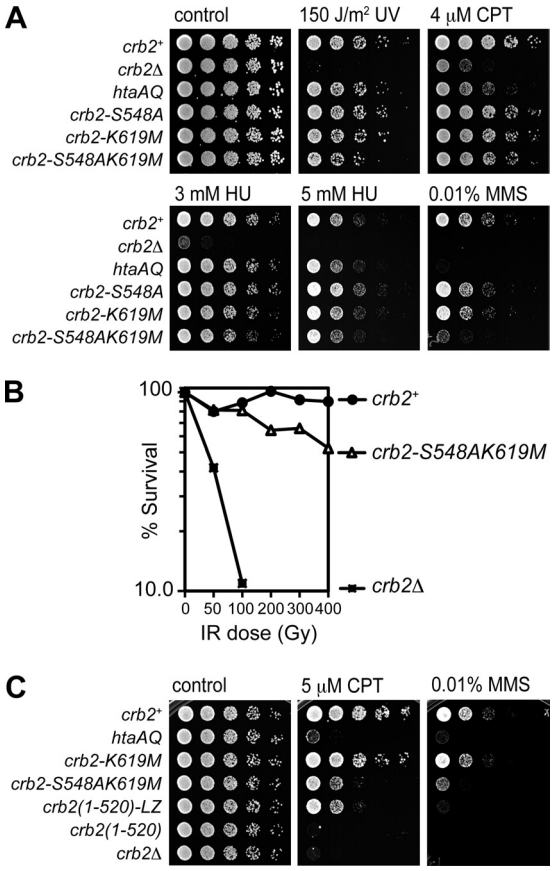

FIG. 3. The Crb2 *S548A* and *K619M* mutations are additive for genotoxin sensitivity. (A) Fivefold serial dilutions of wild-type and mutant strains on YES plates were treated as indicated. (B) IR survival curves showing the sensitivity of *crb2-S548AK619M* compared to the wild type and *crb2*Δ. Log-phase cultures were irradiated and plated in triplicate to determine cell viability. (C) Replacement of Crb2-$BRCT_2$ with a leucine zipper (LZ) dimerization domain leads to genotoxin sensitivity similar to that of *crb2-S548AK619M*. Control plates, UV treatment plates, 3 mM HU, and 4 μM CPT plates were photographed after 2 to 3 days at 30°C. The 5 μM CPT, 5 mM HU, and 0.01% MMS plates were photographed after 3 to 4 days. The strains used for the experiments shown in this figure are LLD3260 (*crb2*$^+$), LLD3259 (*crb2*Δ), LLD4898 (*hta-AQ*), LLD4901 (*crb2-S548A*), LLD4902 (*crb2-K619M*), SAS4908 (*crb2-S548AK619M*), LLD3495 [*crb2*(*1-520*)], and LLD3496 [*crb2*(*1-520*)*-LZ*].

T215A background and challenged cells with a range of genotoxins. In each case we detected negative genetic interactions; i.e., the combined mutants were more sensitive than the individual mutants (Fig. 4A and B). These data show that Thr215 phosphorylation and γ-H2A binding independently affect Crb2 function.

Interestingly, the *crb2-T215AS548A* and *crb2-T215AK619M* strains exhibited sensitivity profiles that were nearly identical to that of *crb2*Δ (Fig. 4A and B), even though our localization data indicate that the individual *S548A* or *K619M* mutations do not fully abolish IRIF formation *in vivo* (Fig. 2). However, we were unable to detect any 2YFP-Crb2 IRIF in *crb2-T215AS548A* and *crb2-T215AK619M* cells (Fig. 4C) (Sofueva and Russell, unpublished). Thus, *S548A* or *K619M* mutations weaken BRCT domain interactions with γ-H2A to such an extent that an intact Thr215 phosphorylation site becomes essential for Crb2 IRIF formation and function.

While *htaAQ*, *crb2-S548A*, or *crb2-K619M* mutations each had negative genetic interactions with *crb2-T215A*, there were some interesting differences between *htaAQ* and the BRCT domain mutations. When challenged with CPT, the *crb2-T215A htaAQ* strain was more sensitive than any other mutant, including *crb2*Δ (Fig. 4A). These data are consistent with γ-H2A having Crb2-independent functions required for CPT resistance, i.e., recruiting Brc1 to damaged replication forks (40). The relationship was reversed at higher doses of IR, with the *crb2-T215A htaAQ* strain being more resistant than *crb2-T215AS548A*, *crb2-T215AK619M*, or even *crb2*Δ (Fig. 4B). These data are consistent with evidence that γ-H2A is detrimental to high-dose IR survival in the absence of Crb2 (23). The partial rescue of *crb2*Δ by *htaAQ* requires Rqh1, a RecQ DNA helicase whose homologs are mutated in patients with Werner, Bloom, and Rothmund-Thomson syndromes, which are characterized by cancer predisposition or accelerated aging. Apparently, γ-H2A interferes with Rqh1-stimulated DSB repair in the absence of Crb2 (23).

Abbreviated checkpoint response in Crb2 γ-H2A-binding mutants. In *S. pombe*, *htaAQ* mutations enhance IR sensitivity of mutants lacking HR proteins, indicating that γ-H2A has recombination-independent roles in the DNA damage response (23). Indeed, the *htaAQ* mutant has a checkpoint maintenance defect, as indicated by an abbreviated division arrest in response to IR (23). The *set9*Δ mutant also has a checkpoint maintenance defect that is genetically epistatic with *htaAQ* (6). To address whether Crb2-$BRCT_2$ interactions with γ-H2A contribute to the checkpoint response, we carried out checkpoint assays with the $BRCT_2$ mutants. We used the *cdc25-22* temperature-sensitive allele to synchronize cells in late G_2 phase, irradiated with 180 Gy IR, and then returned cells to permissive temperature and scored progress through mitosis. Under these conditions, wild-type cells delayed mitosis for ~60 min (Fig. 5A). The *S548A* and *K619M* Crb2-$BRCT_2$ mutants also delayed mitosis, but division resumed ~20 to 30 min earlier than in wild-type cells. In consonance with our other studies, the checkpoint defect was even stronger in *crb2-S548AK619M* cells (Fig. 5A).

These data indicated that Chk1 activation might be impaired in the Crb2 γ-H2A-binding mutants. To address this question, $Rad3^{ATR}$-dependent phosphorylation of Chk1 was assessed by immunoblotting (39). Assays performed with 30 Gy or 120 Gy IR showed that Chk1 phosphorylation was impaired in the Crb2 γ-H2A-binding mutants (Fig. 5B to E). As seen for the other assays, there was an additive effect of combining a γ-H2A binding mutation with *T215A* (Fig. 5D). From these data we conclude that Crb2-$BRCT_2$ binding to γ-H2A is required for a full-fledged checkpoint response.

Crb2-$BRCT_2$ phosphopeptide-binding pocket interactions are restricted to γ-H2A. To investigate whether the Crb2-$BRCT_2$ interacts with proteins other than γ-H2A, we carried out genetic epistasis tests with the $BRCT_2$ mutations and *htaAQ*. The *crb2-K619M* or *crb2-S548AK619M* mutations did not enhance the CPT or MMS sensitivities of *htaAQ* cells, indicating an epistatic relationship (Fig. 6A). Similarly, the *crb2-S548A*, *-K619M*, and *-S548AK619M* mutations did not exacerbate the Chk1 phosphorylation defect of *htaAQ* cells

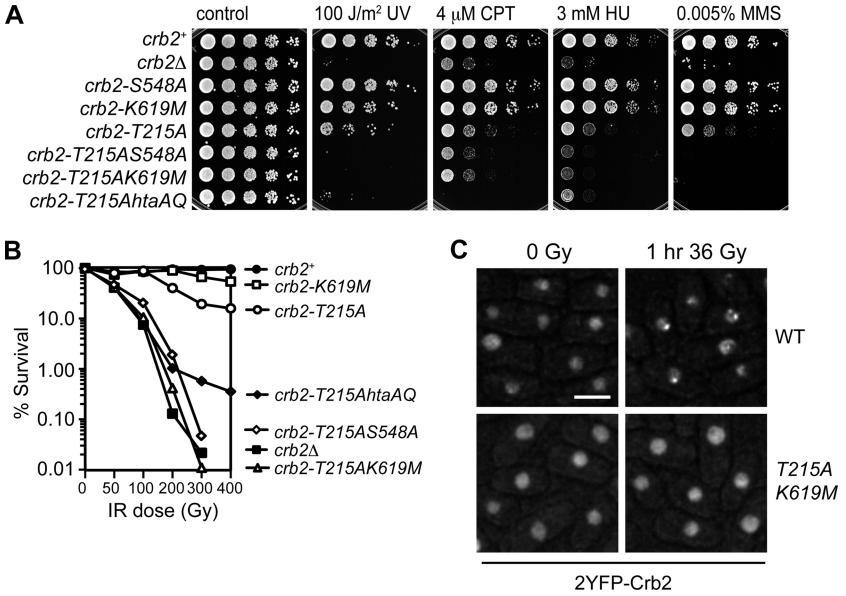

FIG. 4. Mutating Ser548 or Lys619 in the *crb2-T215A* background leads to synergistic sensitivity to genotoxic stress. (A) Abolishing both the histone modification-dependent and -independent pathways of recruiting Crb2 to DNA damage in the *crb2-T215AS548A* and *crb2-T215AK619M* mutants results in a phenotype similar to *crb2*Δ. All plates were photographed after 2 to 3 days at 30°C. (B) IR survival curves confirm strong synergistic interactions of *T215A* with *S548A* or *K619M*. (C) No Crb2 IRIF are detectable in *crb2-T215AK619M* cells. Exponentially growing cultures were irradiated with 36 Gy and photographed 1 h after irradiation. Very similar images were obtained with *crb2-T215AS548A* cells (Sofueva and Russell, unpublished). The strains used for experiments shown in this figure are LLD3260 (*crb2*$^+$), LLD3259 (*crb2*Δ), LLD4901 (*crb2-S548A*), LLD4902 (*crb2-K619M*), LLD4897 (*crb2-T215A*), SAS4903 (*crb2-T215AS548A*), SAS4916 (*crb2-T215AK619M*), and LLD4899 (*crb2-T215A hta-AQ*). WT, wild type. Bar, 5 μm.

(Fig. 6B and C). From these data we conclude that these Crb2-BRCT$_2$ mutations specifically impair binding to γ-H2A, and this is likely the only protein-protein interaction mediated by the BRCT domain phosphopeptide-binding pocket that is important for DNA damage resistance and checkpoint signaling.

Crb2 γ-H2A-binding mutants form foci at DSBs created by the HO endonuclease. Ectopic expression of HO endonuclease in fission yeast cells engineered to have a single HO site can lead to cleavage of both sister chromatids, thereby precluding DSB repair by HR. The resulting DSBs persist and reveal a γ-H2A- and H4-K20me2-independent pathway of forming Crb2 foci. This pathway requires Crb2 Thr215 phosphorylation that mediates an interaction with Cut5 (6). If the Crb2-BRCT$_2$ γ-H2A-binding mutants specifically ablate binding to γ-H2A and do not affect other interactions involving Crb2, they should retain the histone modification-independent pathway of binding DSBs. To test this prediction, we constructed *crb2* mutant strains having a single HO cleavage site near the *arg3* locus and expressing the HO endonuclease from a chromosomally integrated construct regulated by the thiamine-repressible *nmt41* promoter. DSB formation was assessed by microscopic examination of Rad22-2CFP foci (~88 to 96% of cells within a single field had a single focus). As seen before (6), *crb2*$^+$, *crb2-T215A* and *hta-AQ* cells all formed HO-induced Crb2 foci (Fig. 7A). Foci also formed in the *crb2-S548A*, *crb2-K619M*, *crb2-S548AK619M*, *htaAQ crb2-K619M*, and *htaAQ crb2-S548AK619M* mutants, showing that these mutations do not interfere with the histone modification-independent pathway of recruiting Crb2 to DSBs (Fig. 7A). Consistent with our model, HO-induced Crb2 foci were abolished in a *crb2-T215AS548A* strain (Fig. 7B). Quantification of the percent Rad22-2CFP foci that colocalized with 2YFP-Crb2 revealed no differences between wild type and mutants abrogating the histone modification-dependent pathway of Crb2 recruitment (Fig. 7C; Sofueva and Russell, unpublished). In these strains under the conditions used here ~60% of Rad22-2CFP foci overlapped with 2YFP-Crb2. In contrast, the *crb2-T215A* mutation led to an ~4-fold reduction in this value (Fig. 7C). In all cases, nearly all 2YFP-Crb2 foci colocalized with Rad22-2CFP. From these data we conclude that the *crb2-S548A* and *-K619M* mutations specifically ablate the γ-H2A-dependent pathway of recruiting Crb2 to persistent DSBs.

Genetic interactions of Crb2 tudor and BRCT mutations. As previously discussed, microscopically detectable recruitment of Crb2 into IRIF requires the cooperative actions of both the tandem BRCT domains and tandem tudor domains that together constitute the histone modification-dependent pathway of Crb2 recruitment (6, 32). A binding pocket within the tudor domains of Crb2 is important for its interaction with dimethylated H4-K20, the constitutive histone modification created by Set9 methyltransferase and associated with euchromatin (1, 6). Residues within the pocket that participate in the binding interface are Tyr378, Phe400, and Asp402, all of which have direct counterparts in 53BP1 (Tyr1502, Phe1519, and Asp1521, respectively) (1). We have previously shown that mutating the highly conserved Phe400 to alanine disrupts Crb2 IRIF formation and leads to increased genotoxin sensitivity, especially to CPT and UV (6). Similarly, *set9*Δ cells are unable to form Crb2 IRIF and are mildly sensitive to genotoxins (6, 32). Consistent with the tudor domains acting within the histone modification-dependent pathway, combining the *crb2-T215A* mutation with

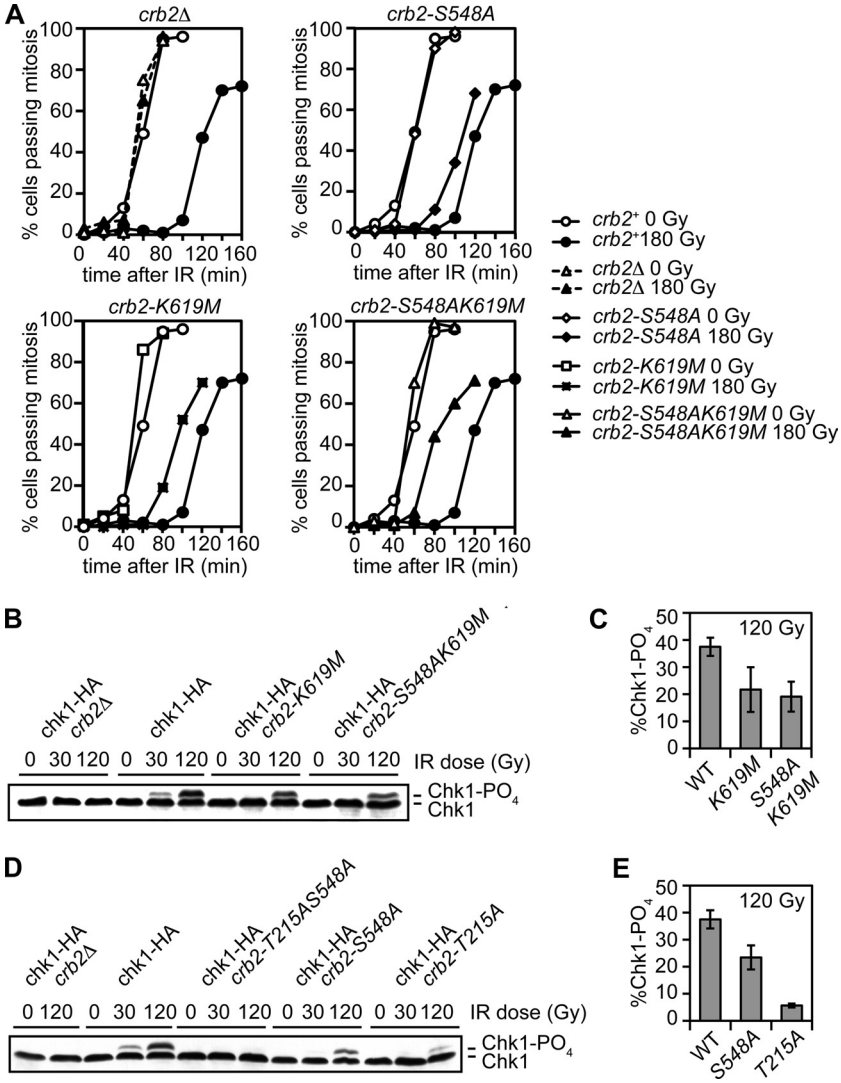

FIG. 5. Crb2-BRCT$_2$ mutants have a defective IR checkpoint response. (A) The checkpoint arrest triggered by IR is abbreviated in *crb2-S548A*, *crb2-K619M*, and *crb2-S548AK619M* cells. The indicated mutants in a *cdc25-22* background were synchronized at late G$_2$ phase by incubation at 35.5°C for 2.5 h. Following 180 Gy IR irradiation, cultures were returned to the permissive temperature of 25°C. Cell division (septation) was assessed by staining cells with Calcofluor. The data shown are representative of multiple experiments. (B) Chk1 phosphorylation is impaired in *crb2-K619M* and *crb2-S548AK619M* mutants. Exponentially growing asynchronous cultures were irradiated with 0, 30, and 120 Gy and harvested immediately following irradiation. (C) ImageJ quantification of the data shown in panel B. (D) Chk1 phosphorylation is ablated in *crb2-T215AS548A* cells. (E) ImageJ quantification of the data shown in panel D. Error bars represent the standard deviations of results from three independent experiments. The strains used for the experiments shown in this figure are SAS4904 (*crb2*$^+$), LLD3628 (*crb2*Δ), SAS4905 (*crb2-S548A*), SAS4906 (*crb2-K619M*), SAS4917 (*crb2-S548AK619M*), SAS4909 (*chk1-HA crb2*Δ), SAS4914 (*chk1-HA crb2*$^+$), SAS4910 (*chk1-HA crb2-S548A*), SAS4911 (*chk1-HA crb2-K619M*), SAS4912 (*chk1-HA crb2-T215AS548A*), SAS4913 (*chk1-HA crb2-S548AK619M*), and SAS4915 (*chk1-HA crb2-T215A*). WT, wild type.

F400A or *set9*Δ results in a strong additive effect and genotoxin sensitivity close to that of *crb2*Δ, while the *set9*Δ *htaAQ* mutant is not more sensitive than either of the single mutants (6, 32).

To further explore the functional relationships of the tudor domains and BRCT domains of Crb2, we performed epistasis studies that assessed the direct consequences of loss of Crb2 binding to γ-H2A and H4-K20me2, rather than loss of the histone modifications themselves. We first compared 2YFP-Crb2 IRIF formation in *crb2-F400A* and *crb2-F400AS548A* cells (Fig. 8A). Both mutants exhibited similar defects (although slightly higher absolute levels) of focus formation to the *crb2-S548AK619M* mutant, indicating that both tudor domain binding to H4-K20me2 and BRCT domain binding to γ-H2A are critical for large-scale localization of Crb2 at repairable DSBs. However, when we compared the genotoxin sensitivities of *crb2-F400AK619M* and *crb2-F400AS548AK619M* mutants to the corresponding mutants defective only in the tudor domain or BRCT domain, we discovered that there was a modest additive effect of combining the tudor and BRCT domain mutations (Fig. 8B). There was a similar modest additive effect when Chk1 phosphorylation was assayed (Fig. 8C to F). These data suggest that the BRCT$_2$-γ-H2A and Tudor$_2$-H4-K20me2 inter-

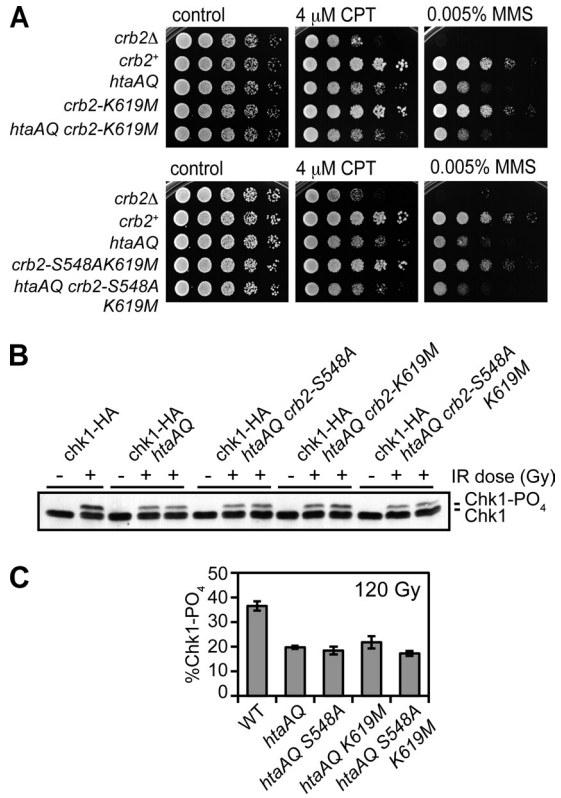

FIG. 6. The Crb2-BRCT$_2$ mutations are epistatic with *htaAQ*. (A) The *htaAQ crb2-K619M* and *htaAQ crb2-S548AK619M* mutants are as sensitive to genotoxins as *htaAQ*. All plates were photographed after 2 to 3 days at 30°C. (B) Chk1 phosphorylation in *htaAQ* is impaired similarly to the Crb2-BRCT$_2$ mutants. Abolishing H2A phosphorylation in the Crb2-BRCT$_2$ mutant backgrounds does not lead to further decrease in Chk1 phosphorylation levels. −, no IR; +, 120 Gy IR. (C) ImageJ quantification of the data shown in panel B. Error bars represent the standard deviations of results from three independent experiments. The strains used for the experiments shown in this figure are LLD3259 (*crb2*Δ), LLD3260 (*crb2*$^+$), LLD4898 (*htaAQ*), LLD4902 (*crb2-K619M*), SAS4921 (*htaAQ crb2-K619M*), SAS4908 (*crb2-S548AK619M*), SAS4920 (*htaAQ crb2-S548AK619M*), SAS4914 (*chk1-HA crb2*$^+$), OL4925 (*chk1-HA htaAQ*), OL4926 (*chk1-HA htaAQ crb2-S548A*), OL4927 (*chk1-HA htaAQ crb2-K619M*), and OL4928 (*chk1-HA htaAQ crb2-S548AK619M*). WT, wild type.

actions can to a partial degree independently affect Crb2 function in checkpoint signaling and DNA damage survival, although both types of interactions are required for full function of Crb2 and its ability to form IRIF. Perhaps the tandem tudor domains are able to recognize multiple histone methylation marks on chromatin, which has also been proposed for the equivalent domains in Rad9 and 53BP1 (1, 12, 17).

DISCUSSION

Crb2 forms IRIF through its interaction with γ-H2A. Although we found that γ-H2A is essential for Crb2 focus formation at IR-induced DSBs (6, 23, 24), Kilkenny et al. (16) detected Crb2 IR-induced foci in a *crb2-K619E* strain harboring a mutation in the γ-H2A-binding pocket of Crb2-BRCT$_2$. These findings suggested an indirect role for γ-H2A in Crb2 IRIF formation; however, we disproved the most obvious model, in which Brc1 binding to γ-H2A is required for Crb2 IRIF formation. Moreover, the weakened interactions between Crb2 and γ-H2A in the *crb2-S548A* and *-K619M* mutants do not reveal a requirement for Brc1 in Crb2 IRIF formation. Having no other well-characterized γ-H2A-binding proteins in fission yeast, we reexamined whether Crb2 binding to γ-H2A is critical for Crb2 focus formation at IR-induced DSBs. Focusing on Ser548 and Lys619, each of which interact directly with the γ-H2A.1 pSer129 phosphate (16), we found that mutations of either residue reduced Crb2 IRIF ~3-fold. Combining the mutations into the same construct reduced Crb2 IRIF to the level of *htaAQ* cells. From these data we conclude that either mutation significantly impairs Crb2 binding to γ-H2A *in vivo*, with full loss of binding occurring in the double mutant. These findings are strikingly similar to our recent analyses of the interactions between phosphothreonine (pThr) residues in the DNA end-processing factor Ctp1 and the FHA domain of the Nbs1 subunit of Mre11-Rad50-Nbs1 (MRN) complex, in which it was necessary to mutate two FHA domain residues that contact pThr to generate a genotoxin-sensitive phenotype (41). Single point mutations of key γ-H2A-interacting residues within the tandem BRCT domain of Crb2 have been shown to fully abrogate the interaction with a phosphorylated peptide derived from H2A.1 *in vitro*; however, we envisage that *in vivo* the high concentration of γ-H2A on chromatin flanking damaged DNA, as well as the multimeric state of Crb2, increases avidity and can explain why single point mutants do not fully abrogate Crb2 IRIF (16). Overall, our data support the hypothesis that large-scale accumulation of Crb2 at IR-induced DSBs requires direct binding to the long tracks of γ-H2A that flank DSBs. This model is consistent with our earlier studies showing that γ-H2A is essential for Crb2 IRIF (6, 23, 24).

Our model fits a common mechanism by which other DNA repair and checkpoint proteins, in particular mammalian Mdc1 and *S. pombe* Brc1, are recruited into microscopically visible foci at sites of DNA damage by directly binding γ-H2A (or γ-H2AX in mammals) through tandem C-terminal BRCT domains (35, 40). Directly analogous residues in the three proteins (Ser548 and Lys619 in Crb2; Thr672 and Lys710 in Brc1; Thr1898 and Lys1936 in Mdc1) form polar interactions with the phosphate group of γ-H2A/X. As revealed perhaps most clearly in the 1.45-Å resolution structure of Brc1 C-terminal BRCT domains bound to a γ-H2A peptide (40), the highly sculpted interactions in the phosphoserine-binding pocket probably contribute to ensuring a sufficient binding affinity for γ-H2A/X despite the modest size of the BRCT protein-phosphoprotein interfaces. Our *in vivo* assays strongly indicate that these phosphoserine interactions cooperate to ensure the assembly of Crb2 into chromatin flanking DSBs. In fact, mutating Mdc1 residues Thr1898 to Val or Lys1936 to Met weakens the protein's binding to a γ-H2AX peptide *in vitro* but does not fully abrogate it (35). This is highly reminiscent of what we see for Crb2 *in vivo*.

Sanders and colleagues (33) have also found that Crb2 binding to γ-H2A is critical for Crb2 IRIF formation. We believe one explanation for the apparent discrepancy between these data and those described in Kilkenny et al. (16) is the difference between imaging of live and fixed cells. In our experience, we have achieved more reproducible and reliable results with

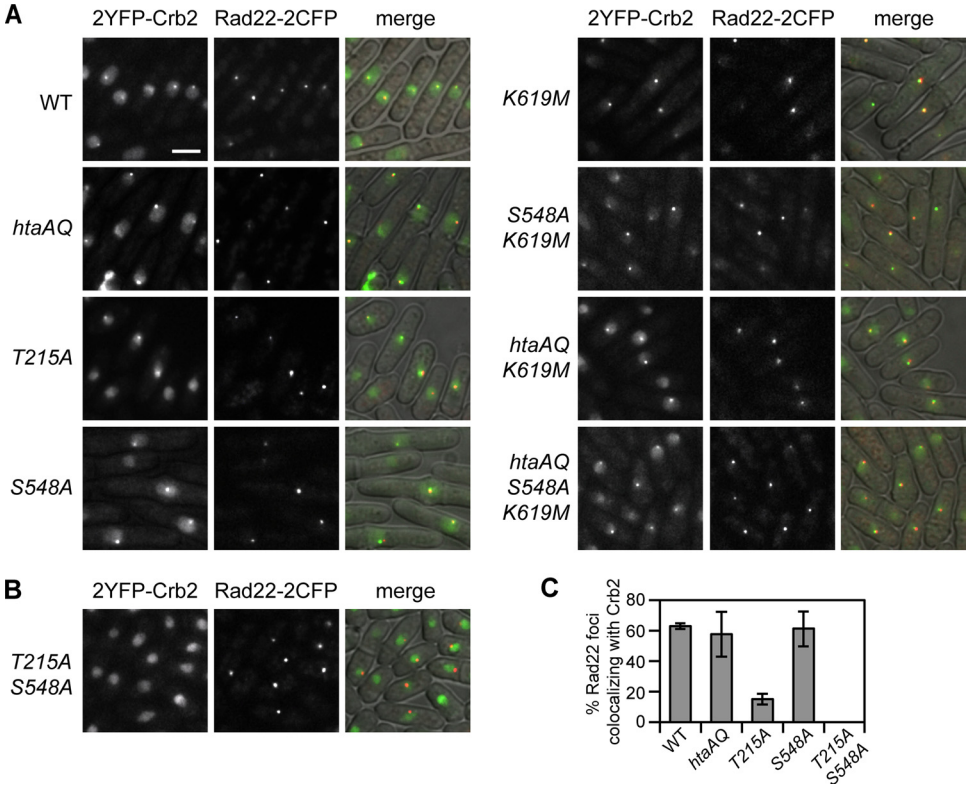

FIG. 7. The Crb2-BRCT$_2$ mutants form foci at DSBs created by the HO endonuclease. Cells carrying the HO cleavage site were grown in the absence of thiamine at 25°C for 27 h, permitting expression of HO. The occurrence of the break was confirmed by visualizing Rad22-2CFP foci (5, 6). (A) As expected, wild-type (WT) or mutant 2YFP-Crb2 impaired in the histone modification-dependent pathway localized to the break site. (B) No Crb2 foci were detected in the *crb2-T215AS548A* mutant, consistent with abrogation of both the histone modification-dependent and -independent pathways of Crb2 recruitment. (C) Quantification of the percentage of Rad22-2CFP foci colocalizing with a 2YFP-Crb2 focus. Nearly all 2YFP-Crb2 foci colocalized with a Rad22-2CFP focus. The strains used are LLD3650 (*crb2*$^+$), LLD3652 (*hta-AQ*), LLD4900 (*crb2-T215A*), SAS4918 (*crb2-S548A*), OL4930 (*crb2-K619M*), OL4931 (*crb2-S548AK619M*), OL4929 (*htaAQ crb2-K619M*), OL4932 (*htaAQ crb2-S548AK619M*), and SAS4919 (*crb2-T215AS548A*).

live cells. Sanders and colleagues also analyzed Crb2 localization in live cells. Fixed-cell analysis of Crb2 localization is potentially more problematic, as indicated by the appearance of focus-like signals that do not overlap with nuclear DNA (16). Our studies also demonstrate the importance of carefully quantifying the effects of mutations in the Crb2-BRCT$_2$ phosphate-binding pocket, as *S548A* and *K619M* mutants were hypomorphs. Quantification of Crb2 foci in the *crb2-K619E* mutant may have revealed a defect (16). In addition, the two methods of visualizing Crb2 IRIF may have different thresholds, and it is formally possible that methanol-fixed-cell analyses cannot discriminate between histone modification-dependent and -independent pathways of recruiting Crb2 to DSBs (6). With these caveats in mind, we conclude that γ-H2A is very likely the only phosphopeptide ligand for Crb2-BRCT$_2$ that is involved in recruiting Crb2 to sites of DNA damage.

Neither *htaAQ* nor *crb2-S548AK619M* mutations completely abrogate Crb2 IRIF. Of the few remaining Crb2 IRIF detected in these cells, we suspect that all form through the histone modification-independent pathway (6), as 2YFP-Crb2 IRIF have not been detected in *crb2-T215AS548A* or *crb2-T215AK619M* cells. Crb2 IRIF in *htaAQ* or *crb2-S548AK619M* cells likely arise from the small fraction of cells that are in G$_1$ phase during IR exposure, as we have previously shown that *htaAQ* cells form Crb2 IRIF when irradiated in G$_1$ phase (6).

To achieve the acute genotoxin sensitivity seen in *crb2*Δ cells, it is necessary to abrogate both histone-modification-dependent and -independent pathways of recruiting Crb2 to DSBs, as in *htaAQ crb2-T215A* cells (6). As predicted by these mechanisms, the genotoxin sensitivity of *crb2-S548AK619M* is relatively mild, being similar to that of *htaAQ* cells. Furthermore, combining *S548A* or *K619M* with *T215A* yields a phenotype equivalent to *crb2*Δ. Thus, the relatively mild phenotype of *crb2-S548AK619M* belies the critical importance of recruiting Crb2 to DNA damage.

The *crb2-S548AK619M* cells were remarkably similar to *crb2*(*1-520*)*-LZ* cells, which encode a Crb2 protein that can artificially homodimerize but cannot bind γ-H2A nor form Crb2 IRIF. In contrast, *crb2*(*1-520*) cells present a null phenotype. These data support the conclusion that Crb2 assembles into homodimers independently of its interactions with the *S548A* or *K619M* mutations and these higher-order structures are absolutely critical for Crb2 function in checkpoint signaling (4, 16).

Dual roles of γ-H2A in maintaining genome integrity. The genotoxin sensitivity of *crb2-S548AK619M* cells is generally

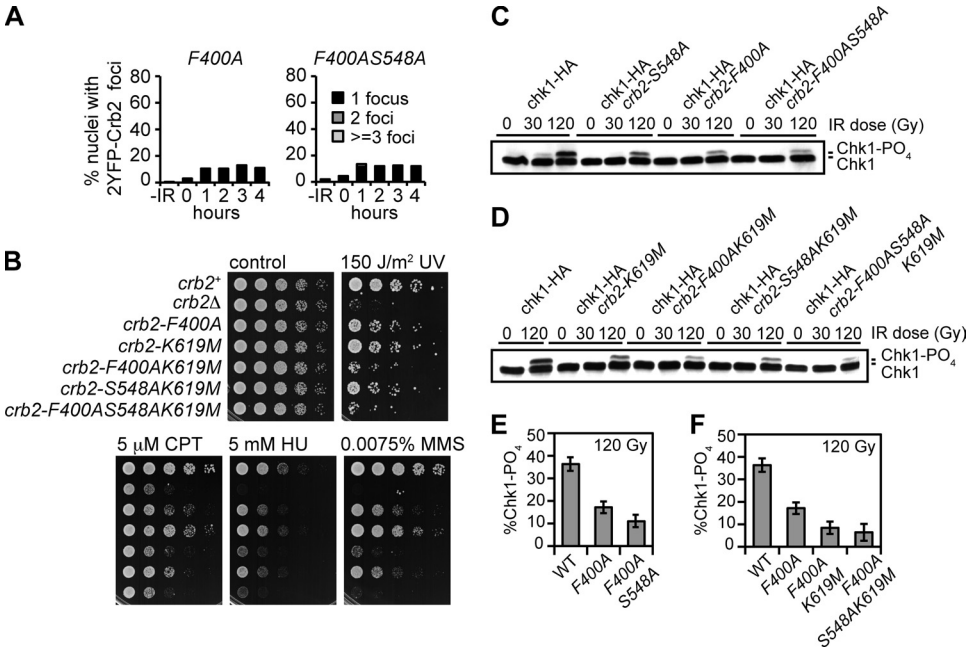

FIG. 8. Genetic interactions of Crb2 tudor and BRCT mutations. (A) Quantification of the percent nuclei with 2YFP-Crb2 foci in *crb2-F400A* and *crb2-F400AS548A* cells. Exponentially growing asynchronous cultures were subjected to 36 Gy IR, and nuclei with 1, 2, or more foci were counted as a percentage of the total. About 200 nuclei were scored for each time point. (B) Epistasis analysis of strains carrying mutations within the tudor and BRCT domains. Control plates, UV treatment plates, 5 μM CPT, and 0.0075% MMS plates were photographed after 2 to 3 days at 30°C. The 5 mM HU plate was photographed after 3 to 4 days. (C and D) Chk1 phosphorylation is further impaired in strains with simultaneously mutated tudor and BRCT domains. (E and F) ImageJ quantification of the data shown in panels C and D. Error bars represent the standard deviations of results from three independent experiments. The strains used for the experiments presented in this figure are LLD3643 (*crb2-F400A*), SAS4942 (*crb2-F400AS548A*), SAS4933 (*crb2*$^+$), LLD3259 (*crb2*Δ), SAS4935 (*crb2-F400A*), SAS4934 (*crb2-K619M*), SAS4936 (*crb2-F400AK619M*), SAS4907 (*crb2-S548AK619M*), SAS4937 (*crb2-F400AS548AK619M*), SAS4914 (*chk1-HA crb2*$^+$), SAS4910 (*chk1-HA crb2-S548A*), SAS4938 (*chk1-HA crb2-F400A*), SAS4939 (*chk1-HA crb2-F400AS548A*), SAS4911 (*chk1-HA crb2-K619M*), SAS4940 (*chk1-HA crb2-F400AK619M*), SAS4913 (*chk1-HA crb2-S548AK619M*), and SAS4941 (*chk1-HA crb2-F400AS548AK619M*). WT, wild type.

similar to that of *htaAQ* cells, which is consistent with equal defects in Crb2 IRIF in the two strains. However, we noted that at higher CPT doses, *htaAQ* cells were more sensitive than the Crb2-BRCT$_2$ mutants, indicating that γ-H2A interacts with other DNA damage response proteins. These findings are consistent with our recent studies showing that γ-H2A binds the C-terminal BRCT domains of Brc1, and mutations in these domains that specifically ablate γ-H2A binding confer sensitivity to CPT (40). We found that Brc1 and Crb2 colocalize in IRIF, but Brc1 also forms spontaneous and HU-induced foci that require binding to γ-H2A. We speculate that chromatin flanking some types of spontaneous or replication-associated DNA damage does not contain or expose H4-K20me2 that interacts with the tudor domains of Crb2, resulting in γ-H2A specifically recruiting Brc1 (40). A critical role for γ-H2A in recruiting both Crb2 and Brc1 to certain types of DNA damage, for example replication fork collapse by CPT poisoning of topoisomerase I, can explain the lower CPT sensitivity of *set9*Δ mutants compared to *htaAQ*, even though both γ-H2A and H4-K20me2 appear to play equally important roles in recruiting Crb2 to chromatin flanking damaged DNA (6).

Crb2 binding to γ-H2A maintains a checkpoint arrest. What role does Crb2 binding to γ-H2A play in survival of DNA damage? We previously found that *htaAQ* cells have an abbreviated IR-induced checkpoint, while the checkpoint is abolished in *htaAQ crb2-T215A* cells (6, 23, 24). From these data we concluded that Crb2 binding to γ-H2A is likely required for a robust and sustained checkpoint response. However, Kilkenny et al. (16) reported that *crb2-K619E* cells have a prolonged checkpoint arrest. They further noted that Rad22 foci persist at slightly higher levels in *crb2-K619E* cells, suggesting a DSB repair defect. Contrary to these findings, we found that checkpoint arrests are shortened in *crb2-S548A*, *-K619M*, or *-S548AK619M* cells. Moreover, we observed no persistence of Rad22 foci in our Crb2 γ-H2A-binding mutants (Sofueva and Russell, unpublished). In agreement with our data, Sanders et al. (33) also found that Crb2 γ-H2A-binding mutants resume division prematurely after exposure to IR. Interestingly, all three studies found that IR-induced Chk1 phosphorylation is diminished in Crb2 mutants that are defective at binding γ-H2A, as we had seen for *htaAQ* mutants (23). Diminished Chk1 phosphorylation is consistent with an abbreviated checkpoint arrest. Thus, the majority of studies support a model in which Crb2 binding to γ-H2A is required for large-scale recruitment of Crb2 to chromatin flanking DSBs, and this is required for efficient phosphorylation of Chk1 by Rad3^{ATR}, which in turn is required for a fully proficient checkpoint arrest.

In budding yeast, phosphorylation of H2A has been implicated in regulation of checkpoint signaling and DNA repair (3, 27, 36). Evidence points to a larger role of γ-H2A in the establishment or maintenance of a transient DNA damage-

induced checkpoint delay in G_1 phase, minor or no involvement in the intra-S-phase checkpoint, and no role in the G_2-M checkpoint that delays progression through mitosis (3, 12, 13, 27). In *Saccharomyces cerevisiae*, γ-H2A and methylation of histone H3-K79 are required for stable retention and focus formation by Rad9 at sites of DNA damage (36). Rad9 binds γ-H2A with a tandem BRCT domain, and mutating Lys1088 within that domain (corresponds to Crb2 Lys619) impairs the G_1 checkpoint activated by IR treatment—a phenotype that is similar to that of an *htaS129** strain that lacks the last four residues of H2A (12). Therefore, γ-H2A interactions with the tandem C-terminal BRCT domains of Rad9 regulate its localization at sites of DNA damage but this is important only for the G_1 phase checkpoint response. It is important to note, however, that some evidence supports a role for Rad9-$BRCT_2$ in checkpoint signaling that is independent of its interaction with γ-H2A, which contrasts with our findings on Crb2 (12, 25).

ACKNOWLEDGMENTS

We thank Claire Dovey for assistance with microscopy, Steven Sanders for discussing data prior to publication, and members of the Russell laboratory and the Scripps Cell Cycle Groups for discussions.

S.S. is supported by a Skaggs-Oxford Scholarship, and L.-L.D. was a fellow of the Leukemia and Lymphoma Society. This work was funded by NIH grants GM59447 and CA77325 awarded to P.R. and CA117638 awarded to J. Tainer/P.R.

REFERENCES

1. **Botuyan, M. V., J. Lee, I. M. Ward, J. E. Kim, J. R. Thompson, J. Chen, and G. Mer.** 2006. Structural basis for the methylation state-specific recognition of histone H4–K20 by 53BP1 and Crb2 in DNA repair. Cell **127:**1361–1373.
2. **Downs, J. A., S. Allard, O. Jobin-Robitaille, A. Javaheri, A. Auger, N. Bouchard, S. J. Kron, S. P. Jackson, and J. Cote.** 2004. Binding of chromatin-modifying activities to phosphorylated histone H2A at DNA damage sites. Mol. Cell **16:**979–990.
3. **Downs, J. A., N. F. Lowndes, and S. P. Jackson.** 2000. A role for Saccharomyces cerevisiae histone H2A in DNA repair. Nature **408:**1001–1004.
4. **Du, L. L., B. A. Moser, and P. Russell.** 2004. Homo-oligomerization is the essential function of the tandem BRCT domains in the checkpoint protein Crb2. J. Biol. Chem. **279:**38409–38414.
5. **Du, L. L., T. M. Nakamura, B. A. Moser, and P. Russell.** 2003. Retention but not recruitment of Crb2 at double-strand breaks requires Rad1 and Rad3 complexes. Mol. Cell. Biol. **23:**6150–6158.
6. **Du, L. L., T. M. Nakamura, and P. Russell.** 2006. Histone modification-dependent and -independent pathways for recruitment of checkpoint protein Crb2 to double-strand breaks. Genes Dev. **20:**1583–1596.
7. **Edwards, R. J., and A. M. Carr.** 1997. Analysis of radiation-sensitive mutants of fission yeast. Methods Enzymol. **283:**471–494.
8. **Esashi, F., and M. Yanagida.** 1999. Cdc2 phosphorylation of Crb2 is required for reestablishing cell cycle progression after the damage checkpoint. Mol. Cell **4:**167–174.
9. **FitzGerald, J. E., M. Grenon, and N. F. Lowndes.** 2009. 53BP1: function and mechanisms of focal recruitment. Biochem. Soc. Trans. **37:**897–904.
10. **Furnari, B., A. Blasina, M. N. Boddy, C. H. McGowan, and P. Russell.** 1999. Cdc25 inhibited in vivo and in vitro by checkpoint kinases Cds1 and Chk1. Mol. Biol. Cell **10:**833–845.
11. **Furnari, B., N. Rhind, and P. Russell.** 1997. Cdc25 mitotic inducer targeted by chk1 DNA damage checkpoint kinase. Science **277:**1495–1497.
12. **Hammet, A., C. Magill, J. Heierhorst, and S. P. Jackson.** 2007. Rad9 BRCT domain interaction with phosphorylated H2AX regulates the G1 checkpoint in budding yeast. EMBO Rep. **8:**851–857.
13. **Javaheri, A., R. Wysocki, O. Jobin-Robitaille, M. Altaf, J. Cote, and S. J. Kron.** 2006. Yeast G1 DNA damage checkpoint regulation by H2A phosphorylation is independent of chromatin remodeling. Proc. Natl. Acad. Sci. U. S. A. **103:**13771–13776.
14. **Kastan, M. B., and J. Bartek.** 2004. Cell-cycle checkpoints and cancer. Nature **432:**316–323.
15. **Keeney, J. B., and J. D. Boeke.** 1994. Efficient targeted integration at leu1-32 and ura4-294 in Schizosaccharomyces pombe. Genetics **136:**849–856.
16. **Kilkenny, M. L., A. S. Dore, S. M. Roe, K. Nestoras, J. C. Ho, F. Z. Watts, and L. H. Pearl.** 2008. Structural and functional analysis of the Crb2-BRCT2 domain reveals distinct roles in checkpoint signaling and DNA damage repair. Genes Dev. **22:**2034–2047.
17. **Kim, J., J. Daniel, A. Espejo, A. Lake, M. Krishna, L. Xia, Y. Zhang, and M. T. Bedford.** 2006. Tudor, MBT and chromo domains gauge the degree of lysine methylation. EMBO Rep. **7:**397–403.
18. **Klein, H. L.** 2008. Molecular biology: DNA endgames. Nature **455:**740–741.
19. **Li, L., and L. Zou.** 2005. Sensing, signaling, and responding to DNA damage: organization of the checkpoint pathways in mammalian cells. J. Cell. Biochem. **94:**298–306.
20. **McGowan, C. H., and P. Russell.** 2004. The DNA damage response: sensing and signaling. Curr. Opin. Cell Biol. **16:**629–633.
21. **Morrison, A. J., J. Highland, N. J. Krogan, A. Arbel-Eden, J. F. Greenblatt, J. E. Haber, and X. Shen.** 2004. INO80 and gamma-H2AX interaction links ATP-dependent chromatin remodeling to DNA damage repair. Cell **119:**767–775.
22. **Moser, B. A., J. M. Brondello, B. Baber-Furnari, and P. Russell.** 2000. Mechanism of caffeine-induced checkpoint override in fission yeast. Mol. Cell. Biol. **20:**4288–4294.
23. **Nakamura, T. M., L. L. Du, C. Redon, and P. Russell.** 2004. Histone H2A phosphorylation controls Crb2 recruitment at DNA breaks, maintains checkpoint arrest, and influences DNA repair in fission yeast. Mol. Cell. Biol. **24:**6215–6230.
24. **Nakamura, T. M., B. A. Moser, L. L. Du, and P. Russell.** 2005. Cooperative control of Crb2 by ATM family and Cdc2 kinases is essential for the DNA damage checkpoint in fission yeast. Mol. Cell. Biol. **25:**10721–10730.
25. **Nnakwe, C. C., M. Altaf, J. Cote, and S. J. Kron.** 2009. Dissection of Rad9 BRCT domain function in the mitotic checkpoint response to telomere uncapping. DNA Repair (Amst.). **8:**1452–1461.
26. **O'Driscoll, M., and P. A. Jeggo.** 2006. The role of double-strand break repair—insights from human genetics. Nat. Rev. Genet. **7:**45–54.
27. **Redon, C., D. R. Pilch, E. P. Rogakou, A. H. Orr, N. F. Lowndes, and W. M. Bonner.** 2003. Yeast histone 2A serine 129 is essential for the efficient repair of checkpoint-blind DNA damage. EMBO Rep. **4:**678–684.
28. **Rhind, N., B. Furnari, and P. Russell.** 1997. Cdc2 tyrosine phosphorylation is required for the DNA damage checkpoint in fission yeast. Genes Dev. **11:**504–511.
29. **Rogakou, E. P., D. R. Pilch, A. H. Orr, V. S. Ivanova, and W. M. Bonner.** 1998. DNA double-stranded breaks induce histone H2AX phosphorylation on serine 139. J. Biol. Chem. **273:**5858–5868.
30. **Rudin, N., and J. E. Haber.** 1988. Efficient repair of HO-induced chromosomal breaks in Saccharomyces cerevisiae by recombination between flanking homologous sequences. Mol. Cell. Biol. **8:**3918–3928.
31. **Saka, Y., F. Esashi, T. Matsusaka, S. Mochida, and M. Yanagida.** 1997. Damage and replication checkpoint control in fission yeast is ensured by interactions of Crb2, a protein with BRCT motif, with Cut5 and Chk1. Genes Dev. **11:**3387–3400.
32. **Sanders, S. L., M. Portoso, J. Mata, J. Bahler, R. C. Allshire, and T. Kouzarides.** 2004. Methylation of histone H4 lysine 20 controls recruitment of Crb2 to sites of DNA damage. Cell **119:**603–614.
33. **Sanders, S. L., A. R. Arida, and F. P. Phan.** 2010. Requirement for the phospho-H2AX binding module of Crb2 in double-strand break targeting and checkpoint activation. Mol. Cell. Biol. **30:**4722–4731.
34. **Strom, L., H. B. Lindroos, K. Shirahige, and C. Sjogren.** 2004. Postreplicative recruitment of cohesin to double-strand breaks is required for DNA repair. Mol. Cell **16:**1003–1015.
35. **Stucki, M., J. A. Clapperton, D. Mohammad, M. B. Yaffe, S. J. Smerdon, and S. P. Jackson.** 2005. MDC1 directly binds phosphorylated histone H2AX to regulate cellular responses to DNA double-strand breaks. Cell **123:**1213–1226.
36. **Toh, G. W., A. M. O'Shaughnessy, S. Jimeno, I. M. Dobbie, M. Grenon, S. Maffini, A. O'Rorke, and N. F. Lowndes.** 2006. Histone H2A phosphorylation and H3 methylation are required for a novel Rad9 DSB repair function following checkpoint activation. DNA Repair (Amst.) **5:**693–703.
37. **Unal, E., A. Arbel-Eden, U. Sattler, R. Shroff, M. Lichten, J. E. Haber, and D. Koshland.** 2004. DNA damage response pathway uses histone modification to assemble a double-strand break-specific cohesin domain. Mol. Cell **16:**991–1002.
38. **van Attikum, H., O. Fritsch, B. Hohn, and S. M. Gasser.** 2004. Recruitment of the INO80 complex by H2A phosphorylation links ATP-dependent chromatin remodeling with DNA double-strand break repair. Cell **119:**777–788.
39. **Walworth, N. C., and R. Bernards.** 1996. rad-dependent response of the chk1-encoded protein kinase at the DNA damage checkpoint. Science **271:**353–356.
40. **Williams, J. S., R. S. Williams, C. L. Dovey, G. Guenther, J. A. Tainer, and P. Russell.** 2010. gammaH2A binds Brc1 to maintain genome integrity during S-phase. EMBO J. **29:**1136–1148.
41. **Williams, R. S., G. E. Dodson, O. Limbo, Y. Yamada, J. S. Williams, G. Guenther, S. Classen, J. N. Glover, H. Iwasaki, P. Russell, and J. A. Tainer.** 2009. Nbs1 flexibly tethers Ctp1 and Mre11-Rad50 to coordinate DNA double-strand break processing and repair. Cell **139:**87–99.
42. **Willson, J., S. Wilson, N. Warr, and F. Z. Watts.** 1997. Isolation and characterization of the Schizosaccharomyces pombe rhp9 gene: a gene required for the DNA damage checkpoint but not the replication checkpoint. Nucleic Acids Res. **25:**2138–2146.